Links:

Locality of Interatomic Interactions in Tight Binding Models for Insulators

Jack Thomas, MASDOC, University of Warwick
Joint work with Huajie Chen & Christoph Ortner

Based on [H. Chen, C. Ortner, J. Thomas. Math. Model. Num., to appear.]
DOI: doi.org/10.1051/m2an/2020020 — ArXiv: arxiv.org/abs/1906.11740

MASDOC
Mathematics and Statistics Centre for Doctoral Training

Motivation

The tight binding model is a simple quantum mechanical model lying, both in terms of computational cost and accuracy, between empirical interatomic potential methods and expensive *ab initio* calculations. Due to the underlying eigenvalue problem, a naive implementation of tight binding models requires $O(N^3)$ computational cost, where N denotes the number of particles in the simulation.

If the quantities of interest in a simulation are mechanical properties, then it may be advantageous to entirely bypass the electronic structure model and replace it with an interatomic potential (IP). The recent transfer of machine learning technology into this domain has made it possible to "fit" high-accuracy IP models, which makes this approach particularly attractive. A starting assumption in most IP models for materials is that the potential energy surface can be decomposed into site energies.

A partial justification for this assumption was given in [2, 3] for linear tight binding models at finite Fermi–temperature. For nuclei positions $y = \{y_n\}$, it was shown that the total potential energy $E(y)$ can be decomposed into exponentially localised site contributions:

$$E(y) = \sum_\ell E_\ell(y), \qquad \text{where} \qquad \left|\frac{\partial E_\ell(y)}{\partial y_n}\right| \lesssim e^{-\eta\,|y_\ell - y_n|} \tag{1}$$

for some $\eta > 0$. The exponent η in (1) measures the interatomic interaction range. Classical IPs are typically fairly short ranged, which is only justified if η is not too small.

Unfortunately, in general, $\eta \sim \beta^{-1}$, where β is the inverse Fermi-temperature. This means that, for moderate to low temperature regimes, the practical value of (1) is limited.

We demonstrate that for insulators, the presence of a spectral gap significantly improves the estimate. Specifically, we show that (1) holds with η independent of β, but instead η is linear in the spectral gap. Moreover, we demonstrate that "pollution" of the spectral gap by a point spectrum caused, for example, by local defects in the crystal, affects only the pre–factors, but not the exponent η in (1).

Tight Binding Model

We take a reference $\Lambda \subset \mathbb{R}^d$ and an atomic configuration $y\colon \Lambda \to \mathbb{R}^d$ satisfying a uniform non–interpenetration condition ($\exists \mathfrak{m} > 0$ s.t. $|y(\ell) - y(k)| \geq \mathfrak{m}$). For a given configuration y, we suppose that the Hamiltonian takes the following form: for $h\colon \mathbb{R}^d \to \mathbb{R}^d$ continuously differentiable, we have

$$\mathcal{H}(y)_{\ell k} \coloneqq h(y(\ell) - y(k)), \qquad \text{where} \qquad |\partial^\alpha h(\xi)| \lesssim e^{-\gamma|\xi|}. \tag{2}$$

While nuclei are treated as classical particles, we assume that electrons are described by a grand canonical potential model (Fermi–temperature, volume and chemical potential, μ, are fixed). For a finite system, we may diagonalise the Hamiltonian ($\mathcal{H}(y)\psi_s = \lambda_s\psi_s$ where $\|\psi_s\| = 1$), and define the grand potential:

$$E^\beta(y) \coloneqq \sum_s \mathfrak{e}^\beta(\lambda_s;\mu) \qquad \text{where} \qquad \mathfrak{e}^\beta(z;\mu) \coloneqq \begin{cases} \frac{2}{\beta}\log\left(1 - f_\beta(z-\mu)\right) & \text{if } \beta < \infty \\ 2(z-\mu)\chi_{(-\infty,\mu)}(z) & \text{if } \beta = \infty. \end{cases} \tag{3}$$

Here, $\beta \coloneqq (k_{\mathrm{B}}T)^{-1}$ is the inverse Fermi–temperature and $f_\beta \coloneqq (1 + e^{\beta\,\cdot})^{-1}$ is the Fermi–Dirac occupation distribution. The zero temperature case ($\beta = \infty$) is defined as the $\beta \to \infty$ limit and is justified in [6].

We may distribute the total energy amongst the atomic sites to obtain a spatial decomposition:

$$E^\beta(y) = \sum_{\ell\in\Lambda} E^\beta_\ell(y) \qquad \text{where} \qquad E^\beta_\ell(y) \coloneqq \sum_s \mathfrak{e}^\beta(\lambda_s;\mu)[\psi_s]^2_\ell. \tag{4}$$

Main Results

For a given configuration y, inverse Fermi–temperature β, and chemical potential $\mu \notin \sigma(\mathcal{H}(y))$, we define the following constants which will determine the interatomic interaction range:

$$\mathsf{d}_\beta \coloneqq \begin{cases} \operatorname{dist}\left(\mu + i\frac{\pi}{\beta}, \sigma(\mathcal{H}(y))\right) & \text{if } \beta < \infty \\ \min\sigma(\mathcal{H}(y)) \cap (\mu,\infty) - \max\sigma(\mathcal{H}(y)) \cap (-\infty,\mu) & \text{if } \beta = \infty. \end{cases} \tag{5}$$

These constants are displayed in Figure 1 for two atomic configurations: a homogeneous lattice, and a point defect configuration (which introduces finitely many additional eigenstates between the bands).

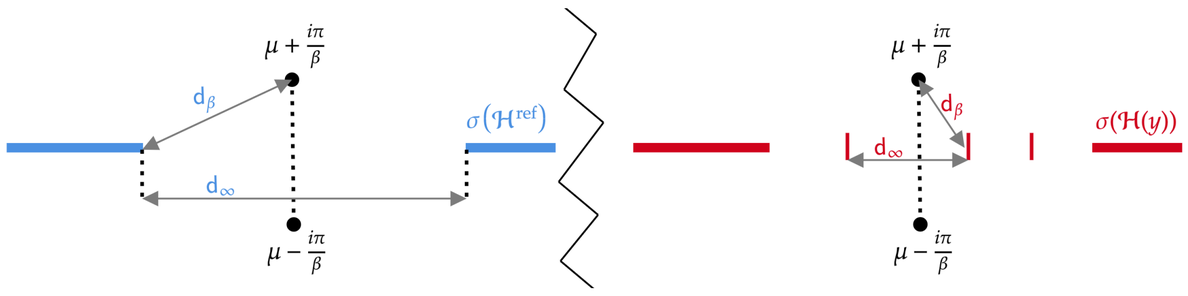

Figure 1: Cartoon depicting the spectrum of the homogeneous (blue) and defect (red) Hamiltonians as well as the corresponding constants d_β from (5).

Theorem 1 *(General Locality Estimates) There exist a constant $\eta_j = \eta_j(\beta)$ such that*

$$\left|\frac{\partial^j E^\beta_\ell(y)}{\partial[y(m_1)]_{i_1}\cdots\partial[y(m_j)]_{i_j}}\right| \leq Ce^{-\eta_j\sum_{l=1}^j |y(\ell)-y(m_l)|} \tag{6}$$

where $\eta_j = c\min\{1, \mathsf{d}_\beta\}$.

Sketch Proof *We write the site energies using resolvent calculus,*

$$E^\beta_\ell(y) \coloneqq -\frac{1}{2\pi i}\oint_{\mathscr{C}} \mathfrak{e}^\beta(z;\mu)\left(\mathcal{H}(y) - z\right)^{-1}_{\ell\ell}\,\mathrm{d}z \tag{7}$$

(for an appropriate contour $\mathscr{C}$) and conclude by applying a standard Combes–Thomas resolvent estimate (and determining the appropriate constants), together with properties of the analytic continuation of $\mathfrak{e}^\beta$.

As depicted in Figure 1 and demonstrated numerically in Figure 2, a point defect introduces finitely many additional eigenvalues between the spectral bands. This means that the constants defined in (5) may become arbitrarily small for low temperatures and thus, by Theorem 1, we obtain locality estimates with arbitrarily small exponents. We may however improve upon these estimates:

Theorem 2 *(Locality Estimates for Point Defects) Let $C^{\mathrm{ref}}, \eta^{\mathrm{ref}}$ be the constants from Theorem 1 when applied to the reference Hamiltonian $\mathcal{H}^{\mathrm{ref}}$. For a point defect configuration y, there exists $C_{\ell m}$ such that*

$$\left|\frac{\partial E^\beta_\ell(y)}{\partial[y(m)]_i}\right| \leq C_{\ell m}e^{-\eta^{\mathrm{ref}}|y(\ell)-y(m)|} \qquad \text{where} \qquad |C_{\ell m} - C^{\mathrm{ref}}| \lesssim e^{-\eta^{\mathrm{ref}}(|\ell|+|m|-|\ell-m|)} \tag{8}$$

with similar estimates for higher derivatives.

Sketch Proof *The Hamiltonian for a system with a point defect can be approximated by a finite rank update of the reference Hamiltonian: $\mathcal{H}(y) \approx \mathcal{H}^{\mathrm{ref}} + P_{\mathrm{FR}}$. We can therefore apply (7) together with the following Woodbury identity:*

$$\left(\mathcal{H}(y) - z\right)^{-1} \approx \left(\mathcal{H}^{\mathrm{ref}} - z\right)^{-1} - \left(\mathcal{H}^{\mathrm{ref}} - z\right)^{-1}\left(I + P_{\mathrm{FR}}\left(\mathcal{H}^{\mathrm{ref}} - z\right)^{-1}\right)^{-1} P_{\mathrm{FR}}\left(\mathcal{H}^{\mathrm{ref}} - z\right)^{-1}.$$

The first contribution results in the improved exponents while the second only increases the pre–factor (but away from the defect core, this pre–factor decays exponentially to the reference pre–factor).

Numerical Experiments

We use the NRL tight binding model [5], implemented in Julia [1], to test the locality in bulk carbon and silicon, both with and without an interstitial defect. Our two test systems are diamond cubic bulk carbon and bulk silicon, which provide ideal test cases of our theory due to their clearly defined band gaps (approximately 0.98 eV for Si and 3.83 eV for C). For both elements, we simulate a supercell model consisting of $5 \times 5 \times 5$ diamond cubic unit cells, containing 1000 atoms in total.

Next, we create a self-interstitial near the origin, and observe the expected pollution of the band gap in the defect system. By adjusting the position of the interstitial, we are able to create configurations where an eigenvalue is arbitrarily close to the Fermi level, creating a challenging situation to confirm our results.

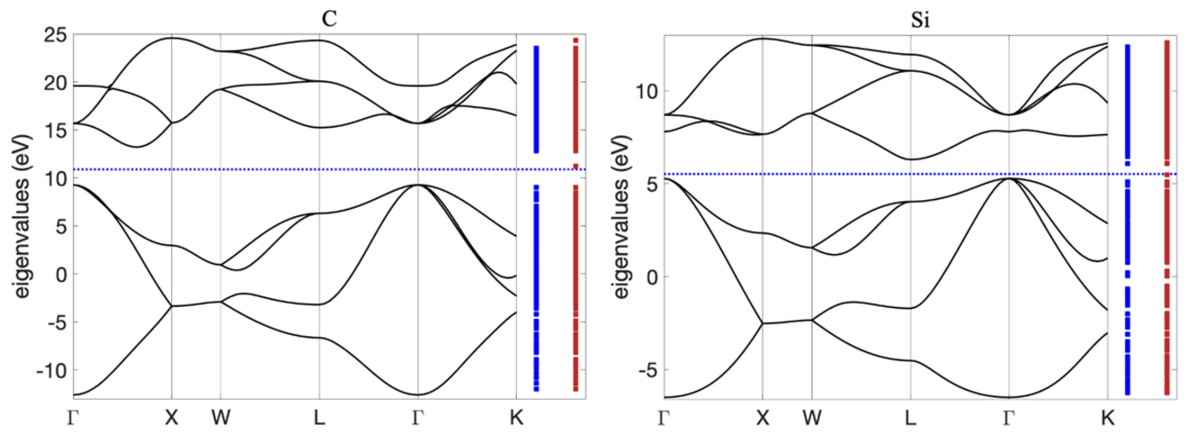

Figure 2: Band structure of C (left) and Si (right).

To test the locality of interatomic interaction we evaluate first and second site energy derivatives and obtain the expected exponential decay. For the defective systems we plot the data points for the interstitial site itself ("$|y|$ small") as well as for the site that has the largest distance to the interstitial atom ("$|y|$ large").

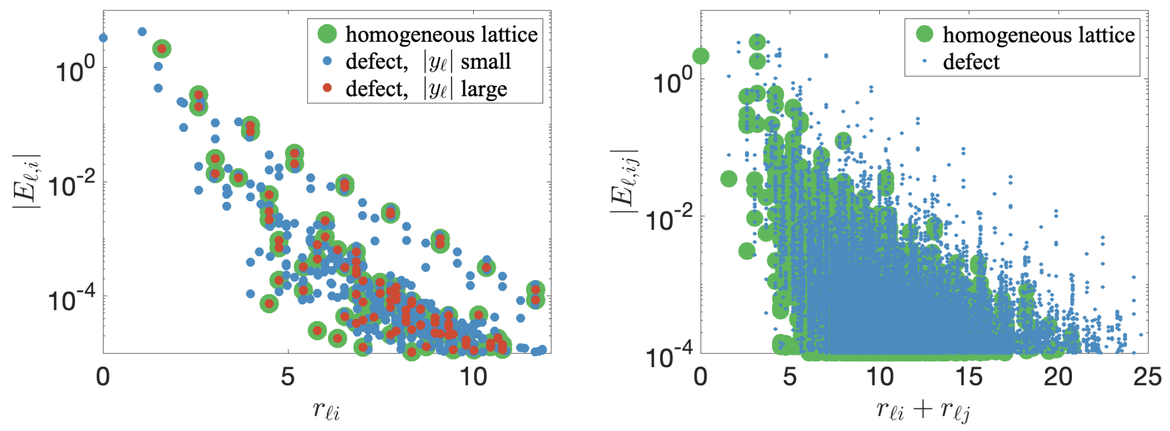

(a) Decay of site energy derivatives. (b) Decay of site energy hessians.

Figure 3: Carbon: Locality of site energies in homogeneous lattice and defect system.

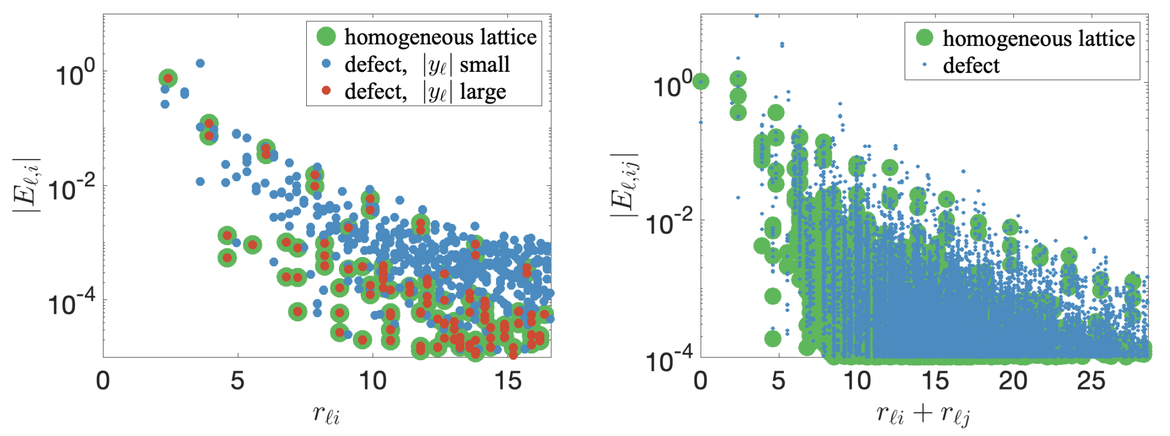

(a) Decay of site energy derivatives. (b) Decay of site energy hessians.

Figure 4: Silicon: Locality of site energies in homogeneous lattice and defect systems.

We clearly observe the exponential decay of interaction strength as predicted in Theorem 1. Moreover, we also observe that for sites far from the defect the site derivative decay perfectly matches that of the bulk system. Two additional observations were unexpected for us: (1) the decay of site derivatives for "near-defect sites" does not exhibit the increased pre–factor that we predicted; however we do see this increase in the second derivatives. (2) the decay of interaction in the silicon system is nearly identical (after rescaling by the lattice constants) to the carbon system even though silicon has a much smaller band gap.

Conclusions

We have described a site energy decomposition for simple linear tight binding models (at both finite and zero Fermi–temperature) and shown that the site contributions are exponentially localised. We have also shown that the exponents in these estimates are independent of the discrete spectrum inside the band gap caused by point defects, and even the pre-factors converge to the pre–factors that would result from using the homogeneous site energy in the estimates, as the distance of a site to the defect increases. Numerical results strongly support our analysis, but also point to possible further extensions.

See [7] for an extension to self–consistent tight binding models.

References

[1] H. Chen and C. Ortner *et al. SKTB.jl.git*. URL: https://github.com/cortner/SKTB.jl.git.

[2] H. Chen, J. Lu, and C. Ortner. "Thermodynamic Limit of Crystal Defects with Finite Temperature Tight Binding". In: *Arch. Ration. Mech. Anal.* 230 (2018), pp. 701–733. DOI: 10.1007/s00205-018-1256-y.

[3] H. Chen and C. Ortner. "QM/MM Methods for Crystalline Defects. Part 1: Locality of the Tight Binding Model". In: *Multiscale Model. Simul.* 14.1 (2016), pp. 232–264. DOI: 10.1137/15M1022628.

[4] H. Chen, C. Ortner, and J. Thomas. "Locality of interatomic forces in tight binding models for insulators". In: *ESAIM: Math. Model. Num.* (to appear). DOI: 10.1051/m2an/2020020.

[5] R.E. Cohen, M.J. Mehl, and D.A. Papaconstantopoulos. "Tight-binding total-energy method for transition and noble metals". In: *Phys. Rev. B* 50 (1994), pp. 14694–14697.

[6] C. Ortner and J. Thomas. "Point defects in tight binding models for insulators". In: *ArXiv e-prints* 2004.05356 (2020). URL: http://arxiv.org/abs/2004.05356.

[7] J. Thomas. "Locality of interatomic interactions in self-consistent tight binding models". In: *ArXiv e-prints* 2004.09323 (2020). URL: http://arxiv.org/abs/2004.09323.